

Behavioral performance modulates spike field coherence in monkey prefrontal cortex

Wei Wu^{a,c}, Diek W. Wheeler^{b,c}, Ellen S. Staedtler^{c,d}, Matthias H.J. Munk^{c,*} and Gordon Pipa^{b,c,*}

^aFrankfurt International Graduate School for Science, ^bFrankfurt Institute for Advanced Studies, Johann Wolfgang Goethe University, ^cMax-Planck-Institute for Brain Research, Deutschordenstr. 46 and ^dDepartment of Anesthesiology, Critical Care and Pain Therapy, Johann Wolfgang Goethe University, Frankfurt, Germany

Correspondence to Gordon Pipa, Max-Planck-Institute for Brain Research, Deutschordenstr. 46, Frankfurt am Main, Hessen, Germany 60528
Tel: +49 69 96769289; fax: +49 69 96769 327; e-mail: pipa@mpih-frankfurt.mpg.de

*Matthias H.J. Munk and Gordon Pipa contributed equally (Gordon Pipa: responsible for the data analysis; Matthias H.J. Munk: responsible for the experimental part)

Received 18 October 2007; accepted 19 November 2007

To investigate neuronal processing during short-term memory, we analyzed behavior-related modulations of coupling between signals on two spatial scales: first, very local multiunit activity and second, local field potentials. Coupling was assessed by spike field coherence using a new approach to overcome limitations in cases of low firing rates. We demonstrate the reliability of our approach with

simulated data. Application to recordings in prefrontal cortex of two monkeys revealed that locking of spikes was differentially modulated with two different frequency bands depending on behavioral performance. *NeuroReport* 19:235–238 © 2008 Wolters Kluwer Health | Lippincott Williams & Wilkins.

Keywords: bootstrapping permutation test, monkey prefrontal cortex, multitaper estimation, oscillations, scale integration, short-term memory spike field coherence

Introduction

Mechanisms of information processing involve neuronal circuits at various spatial scales [1]. Their contributions can be studied by analyzing different signals such as single units, populations of neurons, local field potentials, and other mass signals. Interactions between these different levels are particularly interesting if information processing is subject to behavioral transitions or state changes, even if they are subtle. We tested here whether the relation between synaptic inputs – as reflected in the local field potential – and the spiking output of local neuronal populations in lateral prefrontal cortex changes when perceived information needs to be stored and recalled later in comparison with new sensory input and if these changing relations are the basis for choosing the appropriate behavioral response. As spike field coherence has been shown to change dynamically with memory processing [2–4], we analyzed spike field coherence computed from simultaneously recorded local field potentials and multiunit activity in lateral prefrontal cortex of two monkeys performing a visual short-term memory task. After a baseline of 0.5 s, a sample was presented for 0.5 s, followed by a delay of 3 s. Then, a test stimulus appeared for 2 s, and the monkey had to indicate by differential button press whether the test and sample stimuli matched or not. The primary variable for assessing task-related changes of spike field coherence was behavioral performance, for which we compared trials with erroneous responses to a matched set of trials with correct responses. Spike field coherence was assessed with a multitaper

method [5,6] that allows for an optimal concentration of spectral power and therefore minimizes the problems of leakage. To overcome problems of low spike rate, which can be as low as 1–5 spikes per second in the prefrontal cortex, we developed a combined approach with which we can estimate the reliability of spike field coherence modulations in experimental data as well as quantify the dynamics of the underlying neuronal process. Our approach consists of three steps. In the first step we analyzed performance-related spike field coherence modulations in experimental data. In the second step, we formulated a model for the temporal coordination between the spike and local field potential signals and applied the same analysis as on the experimental data to investigate the reliability of the experimental results. In a third step, we modified the temporal correlation in the model and compared these results with those of the experimental data.

Method

Two adult female rhesus monkeys (*Macaca mulatta*), weighing 6 and 8 kg, were implanted with head bolts and recording chambers over lateral prefrontal cortex mostly ventral of the principal sulcus. All procedures were performed in accordance with German law and NIH guidelines. Eye movements and all behavioral responses were recorded at the same resolution as neuronal signals [7]. We used up to 16 individually movable platinum–tungsten fiber microelectrodes (Thomas Recording, Giessen, Germany)

that were arranged in an array with 500 μm spacing. The spacing of the matrix was chosen to approach the spacing of microcolumns in lateral prefrontal cortex [8]. Signals, digitized at 1 kHz, were preprocessed by rejecting artifacts (movements, licking) and removing line noise at 50 ± 0.5 Hz. Local field potentials and multiunit activities were recorded from the same microelectrodes by employing two band-pass filters (5–150 Hz, 0.5–5 kHz, 3 dB/octave). In total, we could analyze 4124 trials in 12 sessions (1593 pairs) for two monkeys. On average, the monkeys gave correct responses in about 80% of the trials.

Spike field coherence was analyzed in sliding windows (length 200 ms, offset 20 ms) with a multitaper method using four discrete prolate spheroidal sequence tapers of orders 0–3 [5,6]. First, we computed the grand average spike field coherence across all pairs (excluding signal pairs recorded at the same electrode) and all experiments for the frequencies of interest (5–70 Hz, frequency steps 5 Hz). In a second step, we tested the hypothesis that increases and decreases of spike field coherence were performance related. To this end, we used, as the test statistic, the difference $\Delta C_{t,f,p}$ of spike field coherence in correct ('c') and incorrect ('i') trials for each individual sliding window (t), frequency of interest (f), and pair of spike and local field potential signal (p). To derive the statistical significance of $\Delta C_{t,f,p}$, we used a permutation test [9] with 100 permutations of both correct and incorrect trials (H_0 : $\Delta C_{t,f,p}$ is not performance related, test level 1.5%). We then computed for each frequency bin and sliding window the percentage of pairs per session that showed a significant increase in spike field coherence for correct and incorrect responses. To estimate the expected probability of pairs with significant modulation in a given frequency band (band 1: 5–20 Hz and band 2: 25–70 Hz), the results were averaged across sessions and across the respective frequencies of the same band. To allow for variability in the timing and frequencies of states or processes related to behavioral performance across sessions and subjects, time-frequency maps of the results were smoothed with a Gaussian kernel ($\sigma_t=200$ ms/ $\sigma_f=5$ Hz). Smoothed time-frequency maps are referred to as λ -maps. The values λ_c and λ_i describe the percentage of pairs with a significant increase or decrease in spike field coherence for trials with correct and incorrect behavioral responses, respectively. To assess task-related modulation of λ , we derived baseline-corrected modulations by computing the z-score that compares λ during task execution between 0 and 4.5 s to the mean value and the variability during the presample period (–0.5–0 s).

Results of experimental data

During different periods of the task, λ -maps based on spike field coherence revealed values between 0.5 (significance threshold, see below) and 3.5% for different frequency bands. To distinguish these comparatively small changes from spontaneous fluctuations, we z-transformed spike field coherence with respect to the variability during the prestimulus baseline. The time course of the resulting z-scores was modulated in two frequency bands (Fig. 1) and shows remarkable differences for trials with correct and incorrect behavioral responses (compare Fig. 1a and b). The most prominent modulation was observed for the γ frequency band (25–70 Hz) during test stimulus processing and in the early delay of correct trials (λ_c), which yielded

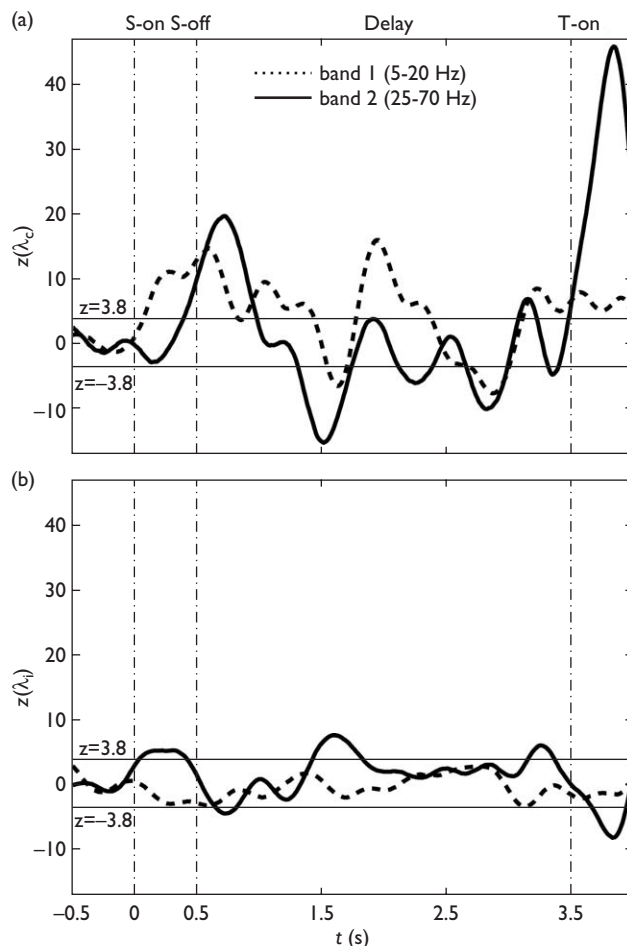


Fig. 1 Time course of performance-related changes of spike field coherence with respect to the pre-sample period. (a) Z-score of average λ_c , which represents the percentage of pairs with robust increases of spike field coherence during correct trials. The dotted line represents the average λ_c value in the frequency band from 5 to 20 Hz, while the solid line represents the average λ_c value in the frequency band from 25 to 70 Hz. (b) Corresponding z-score of average λ_i , for increases of spike field coherence during incorrect trials. Z-values larger than 3.76 and smaller than –3.76 (Bonferroni corrected test level for 1.5% and 170 sliding windows) indicate significant task-related increases and decreases at a 5% significance level, respectively.

z-scores between –15 and more than 40. In contrast, the maximal modulation of λ_i only reached values that were about four times smaller than λ_c .

Although the lower frequencies (5–20 Hz), comprising the classical θ , α , and β bands, were not significantly modulated during error trials, they exhibited a distinct task-related modulation during trials with correct responses. Compared with the modulation of the γ frequencies, low frequencies occurred much earlier in response to sample stimuli, expressed a clear peak in the middle of the delay, and hardly reflected the processing of test stimuli. This demonstrates that modulations in spike field coherence, despite their small values, are highly significant and tightly correlated with the task and the monkey's performance.

Simulated data model and method calibration

To judge the reliability of λ , we generated simulated data comprising exactly the same data structure, that is, the same

number of experiments, trials, and pairs of local field potential and spike signals, and we applied the same analysis as on the experimental data. Further, to investigate the nature of the processes underlying spike field coherence, we modified the temporal correlation of the model and compared the results based on the simulated data and the actual recordings. The local field potential signal was modeled by a sinusoidal oscillation with added white noise of half the oscillation amplitude. To model effects in the low-frequency and high-frequency bands, we generated simulated data containing frequencies (12.5 and 50 Hz) at the centers of the two frequency bands analyzed in the experimental data (see Fig. 1). Spike data were modeled as Poisson processes. To compare the results for simulated and experimental data, we modeled two classes of spike data analogous to trials with correct and incorrect responses. Spike data corresponding to incorrect trials were modeled by a homogenous Poisson process with a spike rate $r_0=5$ spikes/s, which is compatible with the actual experimental spike rate. Spike data corresponding to correct trials were modeled by an inhomogeneous Poisson process based on a spike-rate profile with periods of length w and rate increasing from 5 to $r_1=25$ spikes/s, which then was phase-locked to the local field potential. Spikes induced during these short epochs were phase-locked to the local field potential oscillations if w was small compared with the period length (T) of the oscillation (Fig. 2b). Thus, modifying w enabled us to manipulate spike field coherence based on the modulation of the phase precision. For example, if w is 2 ms for the correct trials of simulated spike data, then the phase precision between the spikes and a 50-Hz local field potential is 0.2π . To model different strengths of synchronization rather than phase precision, we changed the maximal rate modulation r_1 from 25 to 45 spikes/s. Hence, we controlled two parameters that could cause changes of spike field coherence in the simulated data: first, the period width w that modifies the phase precision and second, the difference in r_1 to change the strength of synchronization.

The analysis of the simulated data revealed maximal λ values of 40% for $r_1=25$ and 55% for $r_1=45$ in the low-frequency band 1, which means that the corresponding experimental data with a maximum of 3.5% were far less well locked. The maximum λ values in the high-frequency band 2 amounted to 2.7% and were equal for both $r_1=25$ and $r_1=45$. Increasing w in relation to T ($w > 0.8T$) diminished λ to values of about 0.5% for all models (see, for example, Fig. 2e and f). Nevertheless, the relation of T , w , and the modulation of r_1 interact (Fig. 2c–f) as the decreases of test power were not monotonic with changes of w . Only for the smaller r_1 values and the high-frequency band 2 does test power decrease monotonically as w is increased. At lower frequency band 1, the test power reached its maximum at intermediate values of w (Fig. 2d). The reason for this is that longer windows, which are small compared to T , contain more spikes and are therefore more precisely locked to the local field potential. The average λ and its standard error in the case of H_0 amount to 0.5 and 0.05%, respectively. The average λ is below the test level (1.5%), which indicates a conservative significance. The variability of λ is very low, because of the large number of pairs used. Hence, λ values larger than 0.6 cannot be explained by chance (mean + 2SD). This demonstrates that our new approach is a reliable and sensitive method to detect differences in spike field coherence, even at low spike rates.

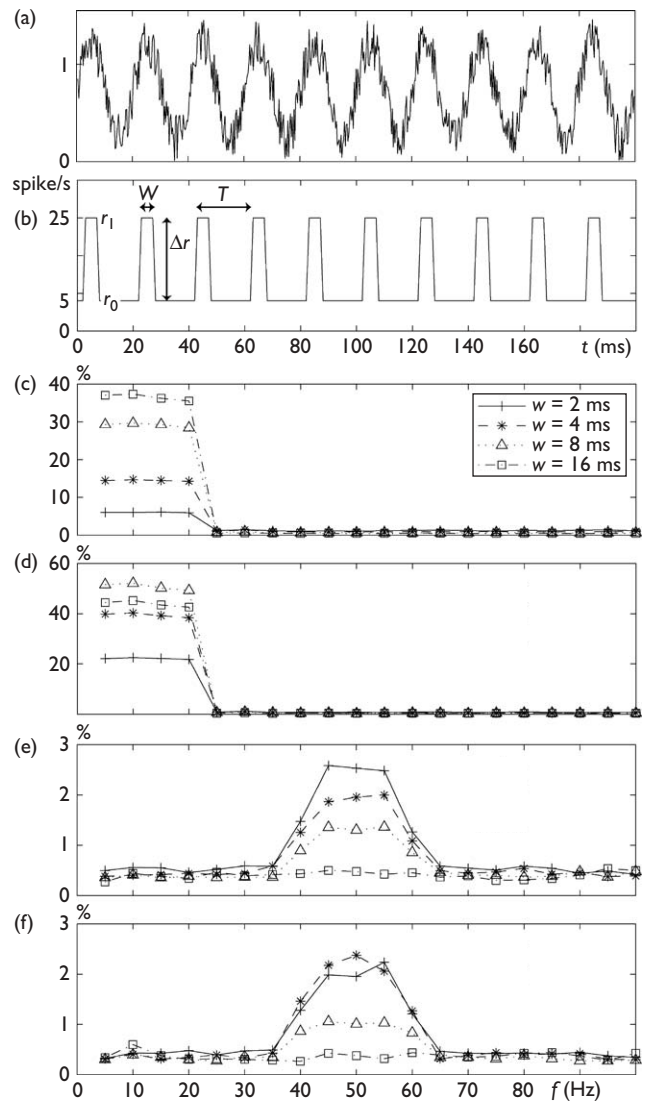


Fig. 2 Test power of simulated data. (a) Local field potential signal composed of a sinusoidal oscillation and additive white noise with amplitude half of the oscillation. (b) The rate profile of spike trains has a strong phase relation with the local field potential signal. (c–f) Test power for spike field coherence between a local field potential and spike signals. [(c) $f=12.5$ Hz, $r_1=25$ spikes/s; (d) $f=12.5$ Hz, $r_1=45$ spikes/s; (e) $f=50$ Hz, $r_1=25$ spikes/s; (f) $f=50$ Hz, $r_1=45$ spikes/s].

Discussion

The value of λ for spike field coherence performance-related differences in the high-frequency band (25–70 Hz) amounted to compatible values for the experimental and simulated data: 3.5 and 2.7%, respectively. The same is true for the average baseline value of λ and its variability in the experimental and simulated data. Therefore, the analysis of both data sets revealed the same maximal relative modulation of λ expressed as a change in z-score of about 40. This demonstrates that even though the variability of individual spike field coherence estimates might be rather large, assessments of performance-related differences of λ on the basis of a large number of estimates is highly reliable. Quantitative comparison of the two types of simulated data, the one modeling phase precision and the other modeling

the strength of synchronization, indicates that experimental results in the high-frequency band are most likely based on precisely phase-locked spikes that have a low probability of occurrence. Given the results from analyzing simulated data, spikes must be locked with a precision of less than 2 ms to local field potential oscillations at 50 Hz (phase precision: 0.2π) to reach λ values close to the maximal values (3.5%) observed in the experimental results. Given the rather short period ($w=2$ ms), however, an oscillation frequency of 50 Hz, and a rate $r_1=25$ spikes/s, we expect 0.5 phase-locked spikes per sliding window on average. This illustrates, first, that the method is very sensitive and second, that differences in spike field coherence due to behavioral performance might be based on rather few synchronous events in prefrontal cortex, which cannot be explained by chance.

Conclusion

Although differences among behavioral conditions appear to be based on rather few instances of phase-locked spikes, the task-related effects on spike field coherence are highly reliable and cannot be explained by chance, as the comparison of results from experimental and simulated data shows. The differential locking of prefrontal neuron populations with two different frequency bands in their input signals suggests that neuronal activity underlying short-term memory in prefrontal cortex transiently engages cortical circuits on different spatial scales, probably in order to coordinate distributed processes.

Acknowledgements

This work was in part funded by the Hertie Foundation (WW, DWW, GP) and the Volkswagen Foundation (MHJM, GP). The authors thank all those who were behind this work.

References

1. Varela F, Lachaux JP, Rodriguez E, Martinerie J. The brainweb: phase synchronization and large-scale integration. *Nat Rev Neurosci* 2001; **2**: 229–239.
2. Pesaran B, Pezaris JS, Sahani M, Mitra PP, Andersen RA. Temporal structure in neuronal activity during working memory in macaque parietal cortex. *Nat Neurosci* 2002; **5**:805–811.
3. Lee H, Simpson GV, Logothetis NK, Rainer G. Phase locking of single neuron activity to theta oscillations during working memory in monkey extrastriate visual cortex. *Neuron* 2005; **45**:147–156.
4. Scherberger H, Jarvis MR, Andersen RA. Cortical local field potential encodes movement intentions in the posterior parietal cortex. *Neuron* 2005; **46**:347–354.
5. Percival DB, Walden AT. *Spectral analysis for physical applications: multitaper and conventional univariate techniques*. Cambridge: Cambridge University Press; 1993.
6. Jarvis MR, Mitra PP. Sampling properties of the spectrum and coherency of sequences of action potentials. *Neural Comp* 2001; **13**:717–749.
7. Bour LJ, van Gisbergen JA, Bruijns J, Ottes FP. The double magnetic induction method for measuring eye movement—results in monkey and man. *IEEE Trans Biomed Eng* 1984; **31**:419–427.
8. Levitt JB, Lewis DA, Yoshioka T, Lund JS. Topography of pyramidal neuron intrinsic connections in macaque monkey prefrontal cortex (area 9 and 46). *J Comp Neurol* 1993; **338**:360–376.
9. Bradley E, Tibshirani RJ. *An introduction to the bootstrap*. London: Chapman & Hall/CRC; 1993.